THE JOURNAL OF BIOLOGICAL CHEMISTRY VOL. 291, NO. 3, pp. 1148–1161, January 15, 2016
Published in the U.S.A.

Bone Morphogenetic Protein-2 (BMP-2) Activates NFATc1 Transcription Factor via an Autoregulatory Loop Involving Smad/Akt/Ca^{2+} Signaling*

Received for publication, June 2, 2015, and in revised form, September 23, 2015 Published, JBC Papers in Press, October 15, 2015, DOI 10.1074/jbc.M115.668939

Chandi C. Mandal[‡1], Falguni Das[§], Suthakar Ganapathy[‡], Stephen E. Harris[¶], Goutam Ghosh Choudhury[§‖2], and Nandini Ghosh-Choudhury[‡‖3]**

*From [‖]Veterans Affairs Research and **Geriatric Research Education and Clinical Center, South Texas Veterans Health Care System and Departments of [‡]Pathology, [§]Medicine, and [¶]Periodontics, University of Texas Health Science Center, San Antonio, Texas 78229*

Background: Mutations in NFATc1 and BMP-2 genes result in bone abnormalities in mice.
Results: BMP-2 activates intracellular Ca^{2+} release, thus activating calcineurin phosphatase to induce NFATc1 expression involving canonical Smad and noncanonical PI 3-kinase in osteoblasts.
Conclusion: BMP-2-stimulated Ca^{2+}-calcineurin-NFATc1 axis potentiates osteoblast differentiation.
Significance: NFATc1 autoregulates its expression in response to BMP-2 in osteoblasts.

Bone remodeling is controlled by dual actions of osteoclasts (OCs) and osteoblasts (OBs). The calcium-sensitive nuclear factor of activated T cells (NFAT) c1 transcription factor, as an OC signature gene, regulates differentiation of OCs downstream of bone morphogenetic protein-2 (BMP-2)-stimulated osteoblast-coded factors. To analyze a functional link between BMP-2 and NFATc1, we analyzed bones from OB-specific BMP-2 knockout mice for NFATc1 expression by immunohistochemical staining and found significant reduction in NFATc1 expression. This indicated a requirement of BMP-2 for NFATc1 expression in OBs. We showed that BMP-2, via the receptor-specific Smad pathway, regulates expression of NFATc1 in OBs. Phosphatidylinositol 3-kinase/Akt signaling acting downstream of BMP-2 also drives NFATc1 expression and transcriptional activation. Under the basal condition, NFATc1 is phosphorylated. Activation of NFAT requires dephosphorylation by the calcium-dependent serine/threonine phosphatase calcineurin. We examined the role of calcium in BMP-2-stimulated regulation of NFATc1 in osteoblasts. 1,2Bis(2aminophenoxy)ethane*N,N,N′,N′*-tetraacetic acid acetoxymethyl ester, an inhibitor of intracellular calcium abundance, blocked BMP-2-induced transcription of NFATc1. Interestingly, BMP-2 induced calcium release from intracellular stores and increased calcineurin phosphatase activity, resulting in NFATc1 nuclear translocation. Cyclosporin A, which inhibits calcineurin upstream of NFATc1, blocked BMP-2-induced NFATc1 mRNA and protein expression. Expression of NFATc1 directly increased its transcription and VIVIT peptide, an inhibitor of NFATc1, suppressed BMP-2-stimulated NFATc1 transcription, confirming its autoregulation. Together, these data show a role of NFATc1 downstream of BMP-2 in mouse bone development and provide novel evidence for the presence of a cross-talk among Smad, phosphatidylinositol 3-kinase/Akt, and Ca^{2+} signaling for BMP-2-induced NFATc1 expression through an autoregulatory loop.

The skeleton provides structural stability for daily activities, and it uniquely responds to mechanical loading and unloading. The mechanical stress signals are translated into physiological responses for sustaining optimum bone quality. Maintenance of skeletal balance relies on bone remodeling coordinated by actions of bone-forming osteoblasts, the mechanical and biological signal-sensing osteocytes, and the bone-resorbing osteoclasts (1). Bone is the major calcium storage organ in the body. Calcium signaling is necessary for differentiation and activity of osteoblasts and osteoclasts (2–4). Osteoclast differentiation is dependent on stromal cell/osteoblast-derived factors, colony-stimulating factor 1 (CSF-1), and receptor activator of NFκB ligand (RANKL)[4] (5). High calcium concentration induces osteoclast formation by increasing RANKL expression (6).

The nuclear factor of activated T cells (NFAT) is involved in calcium-induced RANKL expression in osteoblasts (7). NFATs represent a family of transcription factors that were originally discovered as inducible nuclear factors associated with inter-

* This work was supported in part by Veterans Affairs Merit Review grants and National Institutes of Health Grant RO1 AR52425 (to N. G.-C.) and National Institutes of Health Grant RO1 DK50190 and Veterans Affairs Merit Review grants (to G. G. C.). The authors do not have any conflict of interests. The content is solely the responsibility of the authors and does not necessarily represent the official views of the National Institutes of Health.
[1] Recipient of a Cancer Prevention Research Institute of Texas fellowship. Present address: Dept. of Biochemistry, School of Life Sciences, Central University of Rajasthan, Ajmer 305801, India.
[2] Recipient of a Veterans Affairs Senior Research Career Scientist Award.
[3] To whom correspondence should be addressed: Dept. of Pathology, University of Texas Health Science Center, San Antonio, TX 78229. E-mail: choudhury@uthscsa.edu.

[4] The abbreviations used are: RANKL, receptor activator of NFκB ligand; BMP, bone morphogenetic protein; CsA, cyclosporin A; Ad, adenoviral vector; DN, dominant negative; Luc, luciferase reporter; SBE, Smad binding element; NFAT(c), nuclear factor of activated T cells (cytoplasmic); PI, phosphatidylinositol; BAPTA-AM, 1,2bis(2aminophenoxy)ethane*N,N,N′,N′*-tetraacetic acid acetoxymethyl ester; CSF-1, colony-stimulating factor 1; BMPR, BMP receptor; FRC, fetal rat calvarial bone; qRT-PCR, quantitative RT-PCR; BMP-2 cKO, osteoblast-specific BMP-2-null; Ly, Ly294002; PTEN, *phosphatase and tensin homolog*.

leukin 2 (IL-2) promoter during T cell activation (8). NFATs regulate production of crucial growth factors, cytokines, and cellular proteins that coordinate cell growth and differentiation. There are five members in the NFAT family designated as NFATc1–4, regulated by the intracellular calcium-calmodulin-dependent phosphatase calcineurin and the calcium-independent NFAT5. In resting cells, inactive NFATc1–4 are highly phosphorylated and localized in the cytoplasm. An increase in intracellular calcium concentration activates the serine/threonine phosphatase calcineurin (9). Calcineurin removes critical phosphates from the N terminus of these NFAT proteins, thus exposing a nuclear transport sequence and facilitating their nuclear import (9). Once in the nucleus, NFATs form active transcriptional complexes by pairing with different coactivating proteins. One such partner is identified to be the osteoblastic transcription factor osterix (10). Of the five NFAT isoforms, expression in the mouse osteoblasts is limited to NFATc1 and NFATc3 where NFATc1 regulates NFATc3 expression (7). Calcineurin and NFATc1 control osteoblast proliferation and expression of tartrate-resistant acid phosphatase, the osteoclast-associated receptor cathepsin K, and calcitonin receptor to induce osteoclast differentiation (11–13). NFATc proteins play critical roles in regulating different developmental pathways including bone formation as evidenced by bone formation abnormalities in mice with mutations in NFATc1 and NFATc2 genes (10, 14).

Bone morphogenetic protein-2 (BMP-2) orchestrates osteoblast differentiation and controls osteoclast survival, maturation, and activation by regulating expression of RANKL and CSF-1 (15–20). BMPs signal through type I (BMPR I) and type II (BMPR II) transmembrane receptors. Binding of BMPs to BMPR II recruits BMPR I and activates it by phosphorylation in the GS domain (GS domain consisting of multiple glycin and serine residues) (21, 22). This initiates the intracellular signal transduction by BMPs as the activated BMPR I phosphorylates receptor-activated Smads 1, 5, and 8 that in turn bind to Smad4 and translocate to the nucleus to regulate gene transcription (23, 24). BMP-2 orchestrates integration of Smad signaling with non-Smad signaling in osteoblasts to control their differentiation and gene transcription. A critical role of BMP-2-activated phosphatidylinositol 3-kinase and its downstream partner Akt kinase is established in BMP-2-induced osteoblast differentiation and CSF-1 expression and secretion from osteoblasts to support active osteoclast formation (15, 25). NFATc1 regulates osteoclast differentiation by transcriptionally activating RANKL that feeds back to induce NFATc1 (7, 12, 26). Experimental evidence also suggests a role of NFATc1 in osteoblast-assisted osteoclast activity (13). Both BMP-2 and NFATc1 are essential for driving osteoblast differentiation and osteoblast-mediated osteoclast activity, but a link between these two master regulators of bone remodeling has yet to be described. Here we demonstrate that BMP-2 mobilizes intracellular Ca^{2+} to activate calcineurin phosphatase, leading to NFATc1 transactivation in osteoblasts that in turn leads to autoregulation of NFATc1 gene expression mediated by BMP-2-assisted cross-talk of Smad and PI 3-kinase signaling.

Experimental Procedures

Materials—Recombinant BMP-2 was a gift from Wyeth Pharmaceutical (Cambridge, MA). Tissue culture media, serum, and the nuclear fraction extraction kit (NE-PER) were obtained from Life Technologies. Cell transfection reagent FuGENE HD and luciferase assay kits were purchased from Promega Inc. (Madison, WI). Anti-actin antibody and TRI reagent for RNA isolation were purchased from Sigma. NFATc1, GSK3β, Smad1/5, Smad6, and lamin B antibodies were purchased from Santa Cruz Biotechnology Inc. (Dallas, TX). Phospho-GSK3β and phospho-Smad1/5 antibodies were from Cell Signaling Technology (Danvers, MA).

Cells and Plasmids—C2C12 cells were purchased from ATCC (Manassas, VA). Primary osteoblasts from fetal rat calvarial bone (FRC) were isolated using controlled digestion with trypsin and collagenase (25). C2C12 cells were maintained in DMEM, whereas FRC and murine 2T3 preosteoblast cells (29) were cultured in DMEM or in α-minimal essential medium, respectively, supplemented with 10% fetal bovine serum and 1% penicillin/streptomycin at 37 °C in a humidified atmosphere of 5% CO_2 in air. The confluent cells were serum-starved for 24 h and then treated with varying doses of recombinant BMP-2 in serum-free medium for the indicated periods of time in the presence or absence of different agents. NFATc1 promoter-luciferase constructs were obtained from Dr. Edgar Serfling (University of Wuerzburg, Germany). VIVIT plasmid was purchased from Addgene (Cambridge, MA).

RNA Extraction and Quantitative RT-PCR Analysis—Total RNA was isolated from C2C12 and 2T3 cells in the presence or absence of BMP-2 for the indicated periods of time. If not otherwise described BMP-2 treatment was routinely carried out for 24–48 h. To investigate the signaling mechanism, cells were preincubated with different agents before addition of BMP-2. RNA extraction and quantitative RT-PCR (qRT-PCR) analysis were carried out as described earlier (30–32). In brief, RNA was extracted with TRI reagent. 1 μg of total RNA was reverse transcribed to make cDNA using an RT-PCR First Strand kit (Life Technologies). cDNA was next amplified and quantified in 96-well plates using an ABI Prism 7300 sequence detection system and analyzed by SDS 2.1 software using SYBR Green probe (Applied Biosystems, Foster City, CA). The PCR protocol was as follows: initial denaturation at 94 °C for 10 min followed by 40 cycles at 94 °C for 15 s, annealing at 58 °C for 30 s, and extension at 72 °C for 30 s. PCRs were performed in triplicate for each cDNA and averaged, and the relative mRNA levels were normalized to the reference mouse GAPDH gene (Qiagen, Valencia, CA). NFATc1 primers were used as described by Chuvpilo *et al.* (33).

Transfection and Reporter Assay—Transfection of respective plasmid DNA into cells in 24-well plates was performed with 60–70% confluent cells in serum-free medium as described previously using FuGENE HD according to the manufacturer's protocol (25, 34, 35). Luciferase activity was quantified 24–48 h post-transfection using a luciferase assay kit. The data were plotted as mean luciferase activity/μg of protein as arbitrary units $\pm$S.E.

Immunoprecipitation and Immunoblotting—Cell lysates were prepared using radioimmune precipitation assay buffer (20 mM Tris-HCl, pH 7.5, 150 mM NaCl, 5 mM EDTA, 1 mM Na_3VO_4, 1 mM PMSF, 0.1% protease inhibitor mixture, and 1% Nonidet P-40), and protein concentration was determined using Bio-Rad protein assay reagent. Equal amounts of protein (20–40 μg) were resolved by SDS-gel electrophoresis with or without immunoprecipitation using specific antibodies and transferred to PVDF membrane as described earlier (25, 34, 35). The membranes were incubated for 1 h at room temperature in Tris-buffered saline and 0.1% Tween 20 (TBST) containing 5% (w/v) nonfat dry milk and then treated overnight with primary antibody against NFATc1 (1:200), β-actin (1:5000), tubulin (1:1000), or lamin B (1:1000) in TBST containing 5% bovine serum albumin at 4 °C. Incubation in primary antibody was followed by incubation in the respective secondary antibody labeled with horseradish peroxidase at a 1:20,000 dilution for 1 h at room temperature, and detection of immunoreactive bands was done by HRP-chemiluminescence reagents (Thermo Science). Membranes were reprobed with antibody against β-actin, β-tubulin, or lamin B, which served as loading controls for whole cell lysates, cytoplasmic extracts, or nuclear extracts, respectively.

Electrophoretic Mobility Shift Assay—Nuclear extracts were prepared using the NE-PER kit. The oligonucleotide probe spanning either the Smad binding element (SBE) or the NFATc1 ($NFAT_{tand}$; spanning −700/−661 bp) binding site (33) in NFATc1 promoter was used. The oligonucleotide probe for the putative SBE in NFATc1 promoter spanning the oligonucleotide sequences from −70 to −47 bp in NFATc1 P1 promoter was prepared (Fig. 3*A*). 10 μg of the nuclear extracts were incubated with a radiolabeled SBE probe. The reaction mixture was loaded onto a 5% polyacrylamide gel and resolved by electrophoresis. In supershift analyses, nuclear extracts were preincubated with the indicated antibodies for 15 min at 4 °C followed by addition of radiolabeled probe.

Alkaline Phosphatase Activity—Cells were seeded in 24-well plates at a density of 75,000 cells/well and grown to 90% confluence. The cells were then cultured in osteoblast differentiation medium containing ascorbic acid (100 μg/ml) and β-glycerophosphate (5 mM) for 48 h. Alkaline phosphatase activity was measured in the clear cell lysates prepared by repeated freeze-thaw cycles in 0.5% Triton X-100 using *p*-nitrophenyl phosphate (Sigma) as substrate and were normalized by total protein essentially as described before (25, 29). Representatives of three experiments are shown as the mean ± S.E. of triplicate wells.

Chromatin Immunoprecipitation (ChIP) Assay—The ChIP assay was performed using the reagents and protocol provided in a kit from Active Motif (Carlsbad, CA). The chromatins isolated from the experimental cells were immunoprecipitated with immunoglobulin G (IgG), Smad1/5, or NFATc1 antibody followed by controlled digestion and qRT-PCR as described previously (36).

Mineralized Bone Nodule Formation—Cells were cultured as described above in osteoblast differentiation medium containing ascorbic acid and β-glycerophosphate for 10–12 days. For staining the mineralized nodules, the cells were fixed in ice-cold 70% ethyl alcohol for 1 h at 4 °C, washed with distilled water, and stained for 5 min with a 2% solution of Alizarin Red S, pH 4.0 (Sigma). Plates were dried and photomicrographed.

Calcineurin Phosphatase Assay—Calcineurin phosphatase activity was measured using a colorimetric calcineurin cellular activity assay kit (Calbiochem/EMD Millipore) according to the manufacturer's recommended protocol. Cell lysates were cleared by high speed centrifugation, and the supernatant was desalted by gel filtration. Phosphatase activity was determined in the purified lysates using RII phosphopeptide substrate. The activity was calculated as the difference in absorbance at 620 nm in the presence and absence of the phosphopeptide substrate.

Measurement of Intracellular Calcium—Changes of $[Ca^{2+}]$ in osteoblast cells were determined in cell suspensions using the Ca^{2+}-sensitive fluorescent indicator Fura-2/AM (Molecular Probes) (37). Osteoblast cells grown to 80–90% confluence were harvested by trypsin-EDTA and loaded with 2 μM Fura-2/AM in PBS containing 0.01% BSA by incubating in the dark at 37 °C with gentle agitation for 20 min. 2-ml aliquots of the Fura-2-loaded cells (1.5×10^6 cells/ml) were washed, resuspended in fresh medium, and placed in 4-ml cuvettes. $[Ca^{2+}]$ release was measured using a Deltascan fluorometer (Photon Technology International, Edison, NJ). The excitation ratio 340/380 was analyzed using 340- and 380-nm wavelengths for excitation and 505 nm for emission. Changes in $[Ca^{2+}]$ were measured and indexed by the alterations in the fluorescence ratio 340/380.

Immunofluorescence—Cells were grown in chamber slides, serum-starved, and treated with BMP-2. The cells were washed with PBS, fixed, and stained with NFATc1 antibody followed by incubation with Cy3-tagged donkey anti-rabbit secondary antibody. NFATc1 localization was visualized with a fluorescence microscope (Zeiss).

Immunohistochemical Staining—Femur bones from osteoblast-specific BMP-2-null (BMP-2 cKO) and BMP-2 flx/flx (wild type (WT)) mice were fixed for 48 h in 4% phosphate-buffered formalin at 4 °C followed by decalcification in a mixture of 10% EDTA and 4% phosphate-buffered formalin (2.3:1) for 10 days. Decalcified bones were embedded in paraffin, and 8-μm sections were prepared, dried, deparaffinized, blocked, and incubated with NFATc1 antibody followed by secondary antibody labeling and detection using an Elite ABC kit (Vector Laboratories Inc., Burlingame, CA) with diaminobenzidine as the chromogen.

Statistics—Analysis of variance with Student-Newman-Keuls analysis followed by Tukey comparison test was used to determine the significance of the data. The means ± S.E. of the indicated measurements are shown. A p value of less than 0.05 was considered significant.

Results

BMP-2 Regulates NFATc1 Expression—BMP-2 is critical in osteoblast differentiation. A role for NFATc1 is also implicated in osteoblast cell proliferation and differentiation (10, 13). To test whether BMP-2 regulates NFATc1, we analyzed NFATc1 protein expression in C2C12 cells, which differentiate into osteoblasts in the presence of BMP-2. BMP-2 dose-dependently increased NFATc1 expression (Fig. 1*A*). We found 100 ng/ml

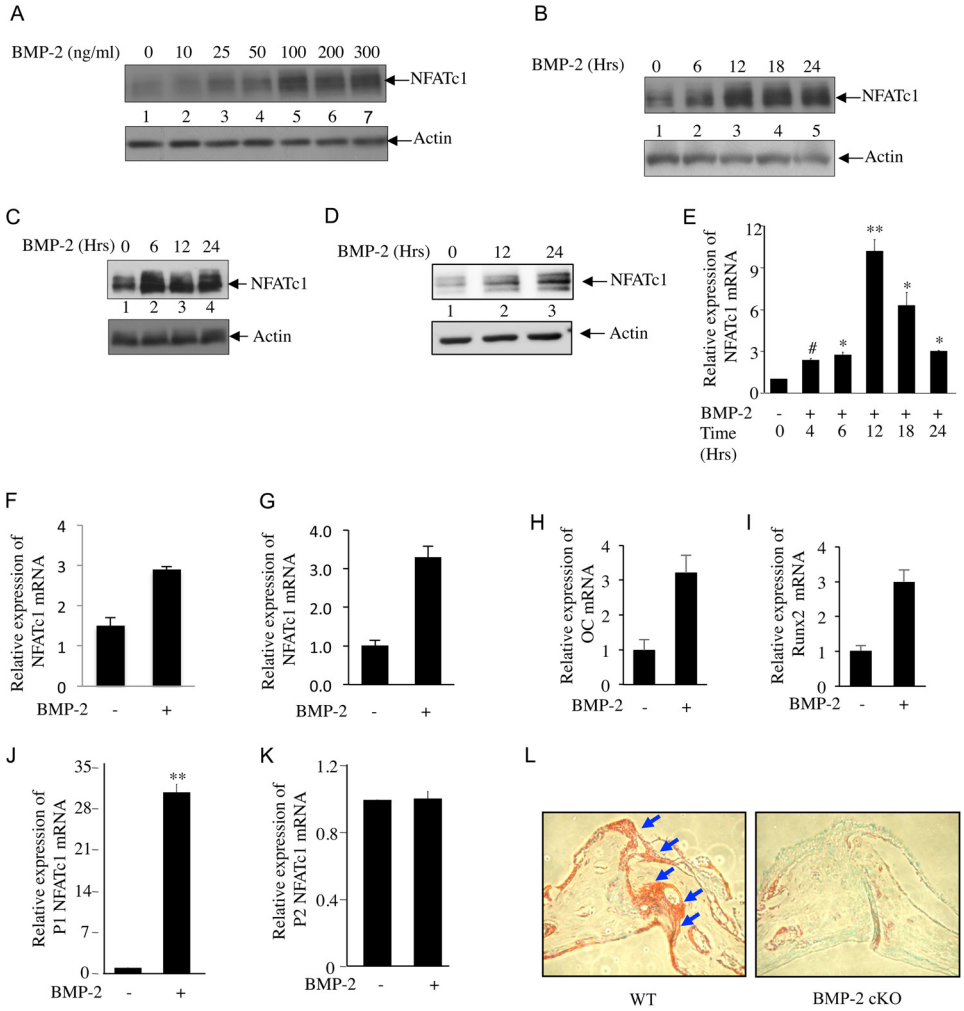

FIGURE 1. **BMP-2 is necessary for NFATc1 expression in osteoblasts.** *A*, BMP-2 dose-dependently increases NFATc1 expression in C2C12 cells. Cells were incubated with increasing doses of BMP-2 (25, 50, 100, 200, and 300 ng/ml) in serum-free medium followed by immunoblotting with antibodies against NFATc1 (*upper panel*) and actin (*lower panel*). *B*, time kinetics for BMP-2-induced NFATc1 expression. C2C12 cells were treated with 100 ng/ml BMP-2 for 6, 12, 18, and 24 h in serum-free medium followed by immunoblotting with NFATc1 and actin antibodies. *C* and *D*, BMP-2 increases NFATc1 protein expression in 2T3 and FRC cells. Cell lysates from 2T3 (*C*) or primary FRC osteoblasts (*D*) treated with BMP-2 for the indicated times were immunoblotted with NFATc1 (*upper panel*) or actin (*lower panel*) antibody. *E*, time kinetics for BMP-2-mediated NFATc1 mRNA expression. RNA was isolated from BMP-2-treated C2C12 cells and analyzed for NFATc1 mRNA expression by qRT-PCR as described under "Experimental Procedures." The mRNA values were normalized to GAPDH expression in the same sample. Mean ± S.E. of quadruplicate measurements is shown. #, $p < 0.05$ *versus* control; *, $p < 0.01$ *versus* control; **, $p < 0.001$ *versus* control. *F–I*, BMP-2 regulates NFATc1 and osteogenic gene expression in osteoblasts. RNA was isolated from 2T3 (*F*), FRC (*G*), or C2C12 (*H* and *I*) cells after BMP-2 treatment for 24 h. Total RNA was used for cDNA preparation followed by analysis of NFATc1 (*F* and *G*), osteocalcin (*OC*) (*H*), or Runx2 (*I*) mRNA expression by qRT-PCR using gene-specific primer sets as described above. *J* and *K*, BMP-2 specifically activates NFATc1 P1 promoter utilization. RNA isolated from BMP-2-treated C2C12 cells was analyzed by qRT-PCR for utilization of P1 (*J*) and P2 (*K*) promoters using specific primer sets as described under "Experimental Procedures." Mean ± S.E. of quadruplicate measurements is shown. *, $p < 0.001$ *versus* control. *L*, NFATc1 expression is inhibited in osteoblast-specific BMP-2-null mice. Bone sections from BMP-2 flx/flx (WT) and BMP-2 cKO mice were immunohistochemically stained for NFATc1 expression. *Error bars* represent S.E.

BMP-2 to be optimum for NFATc1 expression in these cells (Fig. 1*A*, *lane 5*). Also BMP-2 stimulated NFATc1 protein expression in a time-dependent manner. Increased expression was observed at 6 h and was sustained up to 24 h (Fig. 1*B*). Similarly, BMP-2 increased the expression of NFATc1 protein in 2T3 murine osteoblast cells and in primary FRC osteoblast cells (Fig. 1, *C* and *D*, respectively). Furthermore, BMP-2 increased expression of NFATc1 mRNA in a time-dependent manner in C2C12 cells (Fig. 1*E*). Increased expression was observed at 4 h with maximum levels found at 12 h of BMP-2 stimulation (Fig. 1*E*). A similar increase in NFATc1 mRNA expression was observed in 2T3 and FRC cells (Fig. 1, *F* and *G*, respectively). These results indicate a possible transcriptional regulation of NFATc1 by BMP-2 in osteoblast cells. Parallel to NFATc1 expression, BMP-2 stimulated expression of mRNAs for two osteogenic markers, osteocalcin and Runx2 (Fig. 1, *H* and *I*).

In T cells, alternative use of two promoters (P1 and P2) and two poly(A) sites (pA1 and pA2) results in three isoforms (A, B, and C) of NFATc1 transcripts from 11 exons (33). The short isoform A is the most abundant form of NFATc1 in activated T cells and utilizes the distal P1 promoter and proximal pA1 poly(A) site (33). To examine whether there is a preference in promoter utilization by BMP-2 in osteoblasts, we tested expression of NFATc1 mRNA from both these promoters in response to BMP-2. C2C12 cells were incubated with BMP-2, and NFATc1 mRNA expression was quantified using qRT-PCR primers specifically recognizing transcripts from P1 or P2 pro-

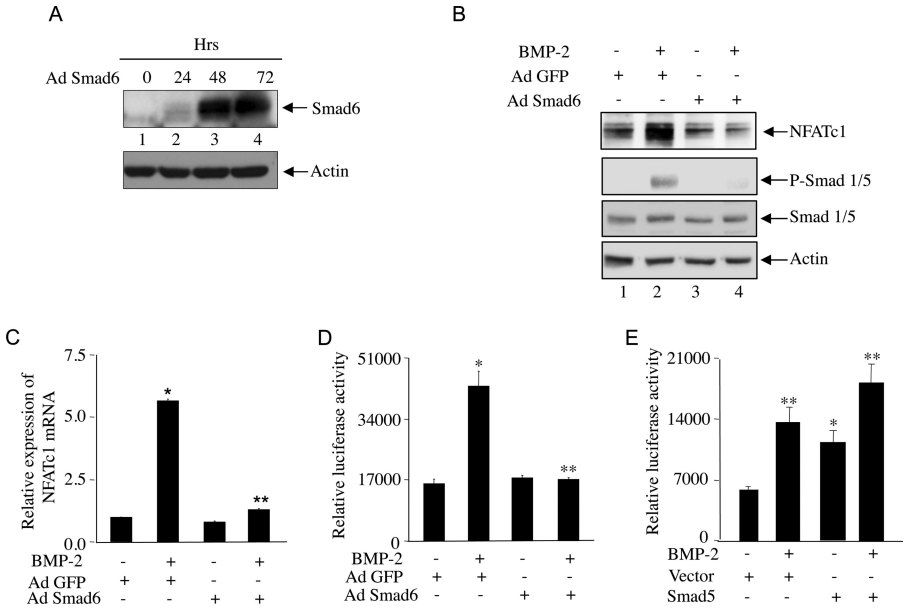

FIGURE 2. **Smad signaling is involved in BMP-2-induced NFATc1 expression.** *A*, Smad6 expression in C2C12 cells treated with adenoviral vector expressing Smad 6 (Ad Smad6). Cells were incubated with Ad Smad6 for 24, 48, and 72 h followed by immunoblotting with Smad6 or actin antibody. *B*, Smad6 blocks BMP-2-induced NFATc1 expression. Cells were preincubated with Ad Smad6 for 48 h followed by BMP-2 treatment. Control cells were preincubated with adenoviral vector expressing GFP (Ad GFP). Cell lysates were immunoblotted with NFATc1, phospho-Smad1/5 (*P-Smad 1/5*), Smad1/5, or actin antibody. *C* and *D*, Smad6 blocks BMP-2-induced NFATc1 mRNA expression (C) and promoter activity (*D*). RNA isolated from C2C12 cells treated as in *B* was analyzed for NFATc1 P1-specific mRNA expression as described in Fig. 1*J*. C2C12 cells were transfected with the 800-bp NFATc1 P1 promoter-driven firefly luciferase construct (NFATc1-Luc) (33) followed by Ad Smad6 or Ad GFP plasmid incubation with or without BMP-2 treatment. Luciferase activities were measured in the cell lysates as described under "Experimental Procedures." In *C*, mean ± S.E. of quadruplicate measurements is shown. *, $p < 0.001$ *versus* control; **, $p < 0.001$ *versus* BMP-2-treated. In *D*, mean ± S.E. of triplicate determinations is shown. *, $p < 0.001$ *versus* control; **, $p < 0.001$ *versus* BMP-2-treated. *E*, C2C12 cells were cotransfected with NFATc1-Luc plasmid and Smad5 expression plasmid or empty vector in the presence or absence of BMP-2. Luciferase activities were measured in the cell lysates. Mean ± S.E. of triplicate determinations is shown. **, $p < 0.001$ *versus* control; *, $p < 0.01$ *versus* control. *Error bars* represent S.E.

moter. BMP-2 significantly enhanced the NFATc1 mRNA expression from P1 promoter in osteoblast cells (Fig. 1*J*), whereas mRNA expression from P2 promoter was found to be non-responsive to BMP-2 treatment (Fig. 1*K*). We used the P1 promoter-driven reporter construct for the remainder of our experiments. To determine whether NFATc1 expression is regulated by BMP-2 *in vivo*, we used tissue sections from a femur of a BMP-2 cKO mouse (38). These mice show reduction in bone mass, radio-opacity, and bone mineral density. Immunohistochemical staining showed significantly reduced NFATc1 expression in BMP-2 cKO mouse bone compared with the BMP-2 flx/flx (WT) mice (Fig. 1*L*).

Smad Signaling Controls NFATc1 Expression—BMP-2 regulates osteoblastic gene expression by signaling through Smad1/5/8, which is inhibited by Smad6. Therefore, we used an adenovirus vector expressing Smad6 to test the involvement of BMP-specific Smad signaling for NFATc1 expression. Infection of C2C12 cells with the vector (Ad Smad6) showed abundant expression of Smad6 at 48 h (Fig. 2*A*). C2C12 cells infected with Ad Smad6 for 48 h were incubated with BMP-2. As shown in Fig. 2*B*, the expression of Smad6 blocked Smad1/5 phosphorylation with a concomitant decrease in BMP-2-induced NFATc1 protein expression (Fig. 2*B*). Similarly, Smad6 blocked BMP-2-induced NFATc1 mRNA expression in these cells (Fig. 2*C*). Furthermore, BMP-2-stimulated transcription of NFATc1 from the P1 promoter was significantly inhibited by Smad6 (Fig. 2*D*). To confirm the involvement of BMP-2-specific Smad in NFATc1 transcription, we tested the effect of Smad5. Expression of Smad5 significantly increased the transcription of NFATc1 to a level similar to levels obtained by BMP-2 treatment (Fig. 2*E*). Both BMP-2 and expression of Smad5 had an additive effect (Fig. 2*E*).

BMP-2 Induces Smad Interaction with NFATc1 Promoter—Analysis of NFATc1 P1 promoter revealed the presence of three SBEs clustered between −70 and −47 bp (Fig. 3*A*). We tested interaction of BMP-specific Smads with NFATc1 promoter using a radiolabeled probe spanning the SBEs (−70/−47 bp) in an electrophoretic mobility shift assay (EMSA). BMP-2 increased DNA-protein complex formation (Fig. 3*B*, compare *lane 2* with *lane 1*). We tested the specificity of DNA-protein interaction using increasing concentrations (1× and 100×) of unlabeled oligonucleotide probe and found reduced formation of DNA-protein complex (Fig. 3*B*, compare *lanes 3* and *4* with *lane 2*). Unlabeled oligonucleotide specific for the transcription factor AP2 did not compete for protein binding to NFATc1 SBE, confirming the specificity of the DNA-protein interaction (Fig. 3*B*, *lane 5*). Interaction of BMP-specific Smads with this SBE region was analyzed by EMSA using Smad-specific antibody. Incubation with antibody specific for Smad1/5 (Fig. 3*C*, *lane 3*), but not the non-immune IgG (Fig. 3*C*, *lane 4*), prior to the addition of radiolabeled probes in the EMSA reaction specifically blocked BMP-2-induced formation of DNA-protein complex. These results indicate specific binding of BMP-specific Smad1/5 with the SBE in the NFATc1 promoter (Fig. 3*C*). Next, using a ChIP assay, *in vivo* association of Smad1/5 with NFATc1 P1 promoter was confirmed (Fig. 3*D*). Importantly, BMP-2 treatment increased Smad1/5 association with NFATc1 P1 promoter as demonstrated in

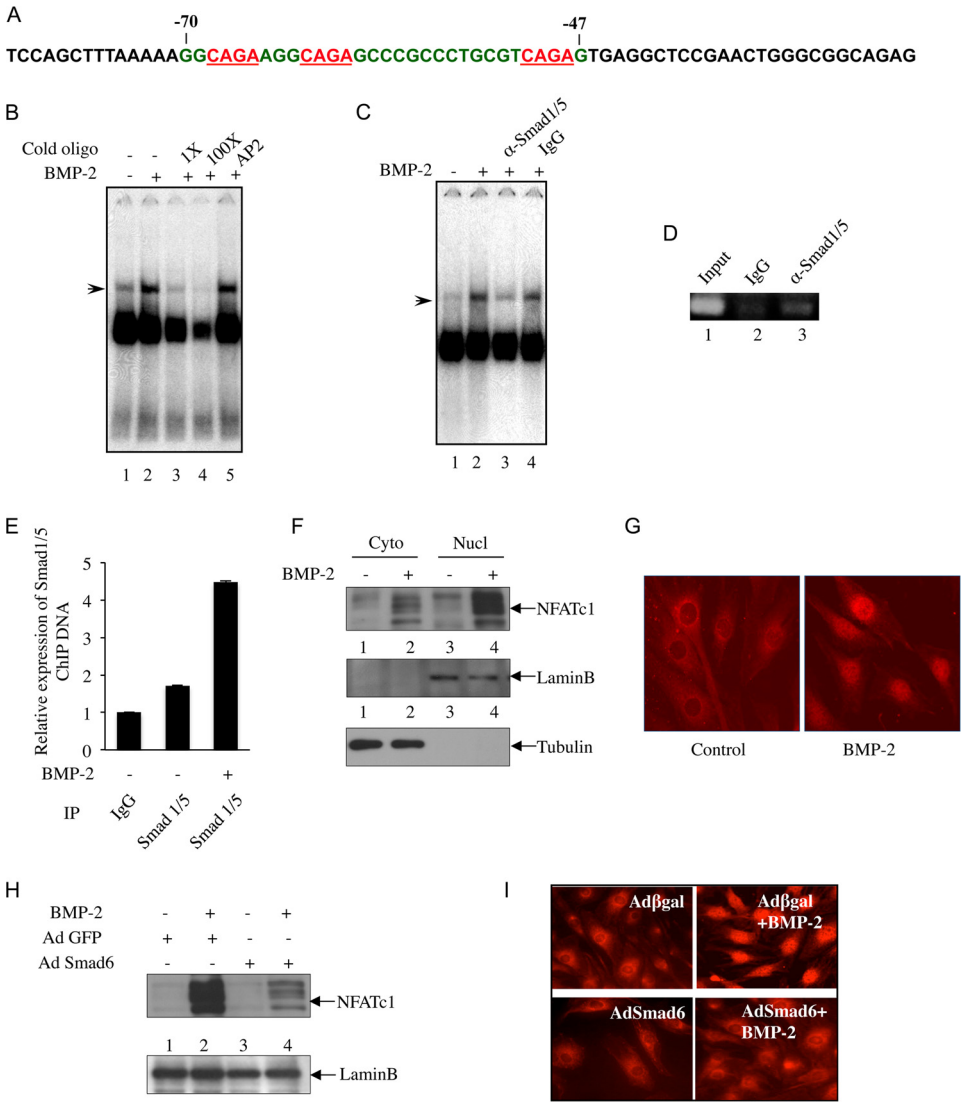

FIGURE 3. **Smad1/5 binds to NFATc1 P1 promoter, and BMP-2/Smad signaling induces NFATc1 nuclear translocation.** *A*, NFATc1 5′ sequences flanking the P1 promoter harboring SBE are shown in *red*. Oligonucleotide spanning −70 to −47 bp (*green*) was used as a probe for EMSA shown in *B* and *C*. *B* and *C*, Smad1/5 binds to NFATc1 P1 promoter. *B*, EMSA was performed using nuclear extracts isolated from C2C12 cells treated with BMP-2 using the radioactive NFATc1 SBE probe described in *A* with or without cold NFATc1 SBE at a 1× (*lane 3*) or 100× (*lane 4*) concentration or a 100× concentration of cold AP2 oligonucleotide with no sequence homology to NFATc1 (*lane 5*). *C*, EMSA was performed with preincubation of nuclear extract with antibody against Smad1/5 (*lane 3*) or IgG (*lane 4*) followed by addition of radioactive NFATc1 SBE probe. *D* and *E*, ChIP assay was performed in C2C12 cells treated with BMP-2 as described under "Experimental Procedures." Transcription factor-chromatin complexes were immunoprecipitated (*IP*) with IgG or Smad1/5 antibody, and DNA fragments were analyzed by PCR and DNA gel analysis (*D*) or qRT-PCR (*E*). *F* and *G*, BMP-2 promotes NFATc1 nuclear import in C2C12 cells. *F*, nuclear (*Nucl*) and cytoplasmic (*Cyto*) fractions were isolated from C2C12 cells treated with BMP-2 and analyzed for NFATc1 expression by immunoblotting using antibody specific for NFATc1 (*top panel*), lamin B (*middle panel*), or tubulin (*bottom panel*). *G*, immunostaining of control and BMP-2-treated cells with NFATc1 antibody. *H* and *I*, Smad6 expression blocks BMP-2-mediated NFATc1 nuclear translocation. Cells were preincubated with Ad Smad6 or Ad GFP followed by BMP-2 treatment, and the nuclear extracts were analyzed for NFATc1 abundance by immunoblotting (*H*). *I*, nuclear translocation of NFATc1 was examined by immunofluorescence. For immunofluorescence, cells were infected with Ad Smad6 or Ad β-gal. *Error bars* represent S.E.

the ChIP assay followed by qRT-PCR using primers spanning the SBEs (Fig. 3*E*).

BMP-2-activated Smad Signaling Is Required for NFATc1 Nuclear Translocation—Our results above show involvement of Smad signaling in BMP-2-induced NFATc1 expression in osteoblast cells. The transcriptional activity of NFATc1 depends on its ability to enter into the nucleus and interact with DNA elements of candidate genes. We analyzed NFATc1 export to the nucleus upon BMP-2 stimulation. BMP-2 significantly increased nuclear localization of NFATc1 (Fig. 3*F*, compare *lane 4* with *lane 3*). We confirmed the ability of BMP-2 to induce NFATc1 nuclear import using immunofluorescence (Fig. 3*G*). Expression of Smad6 reduced BMP-2-induced enrichment of NFATc1 in the nuclear compartment of C2C12 cells, indicating involvement of Smad signaling in NFATc1 nuclear translocation (Fig. 3*H*, compare *lane 4* with *lane 2*). Furthermore, immunofluorescence analysis showed inhibition of BMP-2-stimulated NFATc1 localization by Smad6 (Fig. 3*I*).

Involvement of PI 3-Kinase Signaling in BMP-2-induced NFATc1 Expression—We reported that BMP-2 utilizes PI 3-kinase/Akt signaling to regulate osteoblast differentiation (25).

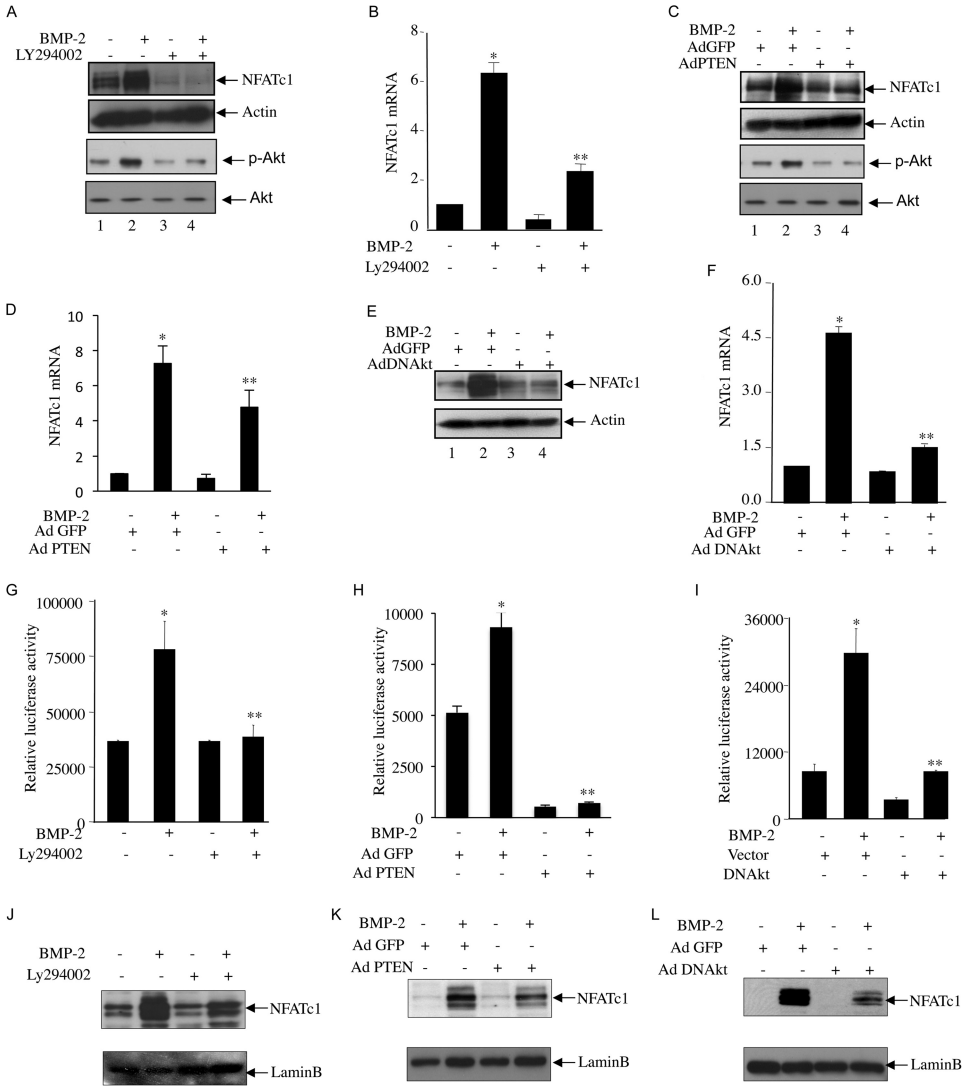

FIGURE 4. **PI 3-kinase/Akt signaling regulates BMP-2-induced NFATc1 protein and mRNA expression, promoter activation, and nuclear translocation.** *A–F*, NFATc1 protein (*A*, *C*, and *E*) and mRNA (*B*, *D*, and *F*) expression was determined in C2C12 cells treated with BMP-2 with or without pretreatment with 12.5 μM Ly294002 (*A* and *B*) or in the presence or absence of adenoviral vectors expressing PTEN (Ad PTEN) (*C* and *D*) or dominant negative Akt (Ad DNAkt) (*E* and *F*). Immunoblotting with NFATc1 or actin antibody (*A*, *C*, and *E*) or qRT-PCR (*B*, *D*, and *F*) was performed. Immunoblotting with phosphorylated Akt (*p-Akt*) and Akt antibodies was performed in cell lysates treated with Ly294002 or infected with Ad PTEN (*A* and *C*). *G–I*, C2C12 cells were transfected with NFATc1-Luc plasmids with or without pretreatment with Ly294002 (*G*), Ad PTEN (*H*), or Ad DNAkt (*I*) with or without BMP-2 treatment. Luciferase activities were measured as described in Fig. 2*D*. For *B*, mean ± S.E. of quadruplicate measurements is shown. *, $p < 0.001$ *versus* control; **, $p < 0.001$ *versus* BMP-2-treated. For *D* and *F*, mean ± S.E. of quadruplicate measurements is shown. *, $p < 0.01$ *versus* control; **, $p < 0.01$ *versus* BMP-2-treated. For *G*, *H*, and *I*, mean ± S.E. of triplicate determinations is shown. *, $p < 0.01$ *versus* control; **, $p < 0.001$ *versus* BMP-2-treated. *J–L*, nuclear fractions were isolated from C2C12 cells treated with Ly294002 (*J*) or incubated with Ad PTEN (*K*) or Ad DNAkt (*L*). Immunoblotting was performed using antibody against NFATc1 (*top panels*) or lamin B (*lower panels*). *Error bars* represent S.E.

To determine the involvement of PI 3-kinase in the BMP-2-mediated increase in NFATc1 protein expression, we used Ly294002 (Ly), a pharmacological inhibitor of PI 3-kinase. Pretreatment of the cells with Ly significantly inhibited BMP-2-induced NFATc1 protein expression in parallel to the inhibition of Akt phosphorylation, a downstream target of PI 3-kinase, indicating involvement of PI 3-kinase signaling (Fig. 4*A*). Ly significantly blocked BMP-2-stimualted NFAT mRNA expression (Fig. 4*B*). PTEN is a specific phosphatase that blocks PI 3-kinase signaling (39). Expression of PTEN blocked phosphorylation of Akt and inhibited expression of NFAT protein and mRNA in response to BMP-2 (Fig. 4, *C* and *D*). We have shown previously that Akt regulates BMP-2-induced osteoblast differentiation (25). Expression of dominant negative Akt kinase attenuated BMP-2-stimuated NFATc1 protein mRNA expression (Fig. 4, *E* and *F*). Similarly, Ly and expression of PTEN or dominant negative Akt significantly decreased the BMP-2-induced transcription of NFATc1 (Fig. 4, *G*, *H*, and *I*). We described above that BMP-2 increased translocation of NFATc1 into the nucleus (Fig. 3, *F* and *G*); therefore, we tested the role of PI 3-kinase/Akt signaling in nuclear localization of NFATc1. Both Ly and PTEN inhibited the BMP-2-stimulated NFATc1 import to the nucleus (Fig. 4, *J* and *K*). Similarly, expression of dominant negative Akt suppressed the nuclear localization of NFATc1 by BMP-2 (Fig. 4*L*). Together, our results demonstrate that PI 3-kinase-dependent Akt kinase regulates BMP-2-mediated expression of NFATc1 and its nuclear translocation.

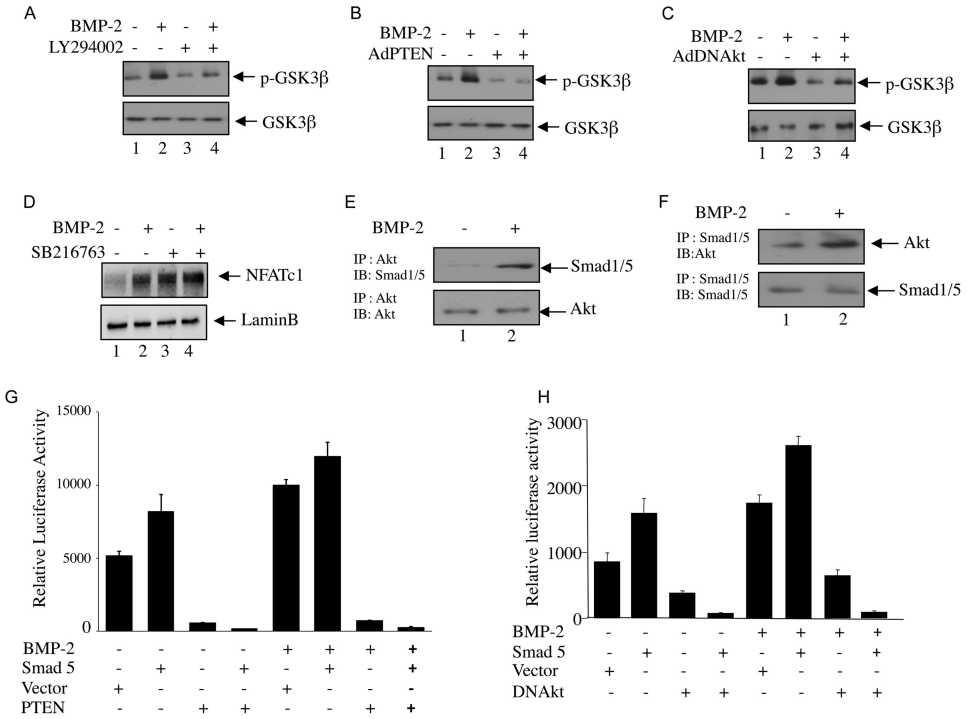

FIGURE 5. **Akt kinase and GSK3β regulate BMP-2-induced NFATc1 expression.** *A–C*, C2C12 cells were treated with Ly294002 (*A*) or infected with adenovirus expressing PTEN (Ad PTEN; *B*) or dominant negative Akt kinase (Ad DNAkt; *C*) before BMP-2 treatment. Cell lysates were immunoblotted with phospho-GSK3β (*p-GSK3β*) (*upper panel*) or GSK3β (*lower panel*) antibody. *D*, C2C12 cells were treated with 25 μM SB216763 prior to incubation with BMP-2. The nuclear lysates were immunoblotted with NFATc1 (*upper panel*) or lamin B (*lower panel*) antibody. *E* and *F*, Akt interacts with Smad1/5. Lysates of C2C12 cells treated with BMP-2 were immunoprecipitated (*IP*) with Akt (*E*) or Smad1/5 (*F*) antibody. The immunoprecipitates were immunoblotted (*IB*) with Smad1/5 (*E*) or Akt (*F*) antibody, respectively. *G* and *H*, Akt and Smad cooperate for NFATc1 transcription. C2C12 cells were cotransfected with NFATc1-Luc plasmid and empty vector or plasmids expressing Smad5 and PTEN (*G*) or Smad5 and a dominant negative form of Akt kinase (DNAkt) (*H*). Cells were incubated with BMP-2, and luciferase activities were measured in the cell lysates as described in Fig. 2. *Error bars* represent S.E.

BMP-2-stimulated Akt Kinase Inactivates GSK3β and Blocks NFATc1 Nuclear Export—GSK3β has been shown to phosphorylate NFATc1 at selected serine residues, and facilitate its exit from nucleus thereby reducing its transcriptional activity (27). Akt conversely can phosphorylate and inactivate GSK3β (28). In an effort to find out the underlying mechanism of Akt-induced activation of NFATc1, we first tested GSK3β inactivation in response to BMP-2 in osteoblast cells. BMP-2 treatment induced phosphorylation of GSK3β (Fig. 5, *A–C*). Inactivation of Akt kinase activity by pretreatment with Ly294002 and expression of PTEN and the dominant negative form of Akt blocked BMP-2-induced GSK3β phosphorylation (Fig. 5, *A–C*). To examine the role of GSK3β in NFATc1 nuclear export in osteoblasts, we examined nuclear localization of NFATc1 in the presence of a pharmacological inhibitor of GSK3, SB216763. Treatment of osteoblasts with SB216763 increased nuclear localization of NFATc1 under the basal condition (Fig. 5*D*, compare *lanes 1* and *3*). However, BMP-2-mediated localization of NFATc1 to the nucleus was not further increased by this treatment (Fig. 5*D*, compare *lanes 2* and *4*). These results indicate that Akt-mediated inactivation of GSK3β may increase the nuclear abundance of NFATc1 to enhance its transcriptional activity in osteoblasts.

BMP-2 Induces Interaction of Akt and Smad1/5 to Initiate Cross-talk between These Two Signaling Pathways—We have shown above that BMP-2-induced NFATc1 transcription involves Smad signaling and Akt signaling pathways (Figs. 2–4). To test the possible existence of cross-talk between these two signaling pathways, we first tested whether Smad1/5 and Akt interact with each other in osteoblasts. Lysates of BMP-2-treated cells were immunoprecipitated with Akt antibody followed by immunoblotting with Smad1/5 antibody. The results show that BMP-2 increased the association between Akt and Smad1/5 (Fig. 5*E*). Reciprocal immunoprecipitation and immunoblotting experiments showed similar results (Fig. 5*F*). These results indicate a possible cross-talk between Akt and Smad1/5. To determine the involvement of this cross-talk, we examined the transcriptional activation of NFATc1 using the reporter construct. NFATc1 promoter was transfected with Smad5 and/or PTEN expression vector. The transfected cells were incubated with BMP-2. As shown in Fig. 5*G*, both BMP-2 and Smad5 increased the transcription of NFATc1. Expression of PTEN, which inhibits the Akt kinase activity, significantly blocked BMP-2-as well as Smad 5-induced transcription of NFATc1 (Fig. 5*G*). Similarly, expression of dominant negative Akt kinase inhibited NFATc1 transcription in response to BMP-1 and Smad5 (Fig. 5*H*). These results indicate the requirement of concerted action of Akt and Smad signaling in BMP-2-induced NFATc1 promoter activation.

BMP-2 Mobilizes Intracellular Ca^{2+} to Induce Calcineurin Activity and Osteoblast Differentiation—NFATc1 activation and nuclear localization require Ca^{2+}-mediated activation of calcineurin phosphatase. We first examined the effect of BMP-2 on Ca^{2+} mobilization. Incubation of C2C12 cells with BMP-2 transiently increased the release of intracellular Ca^{2+} (Fig. 6*A*) that was abrogated upon pretreatment of the cells with

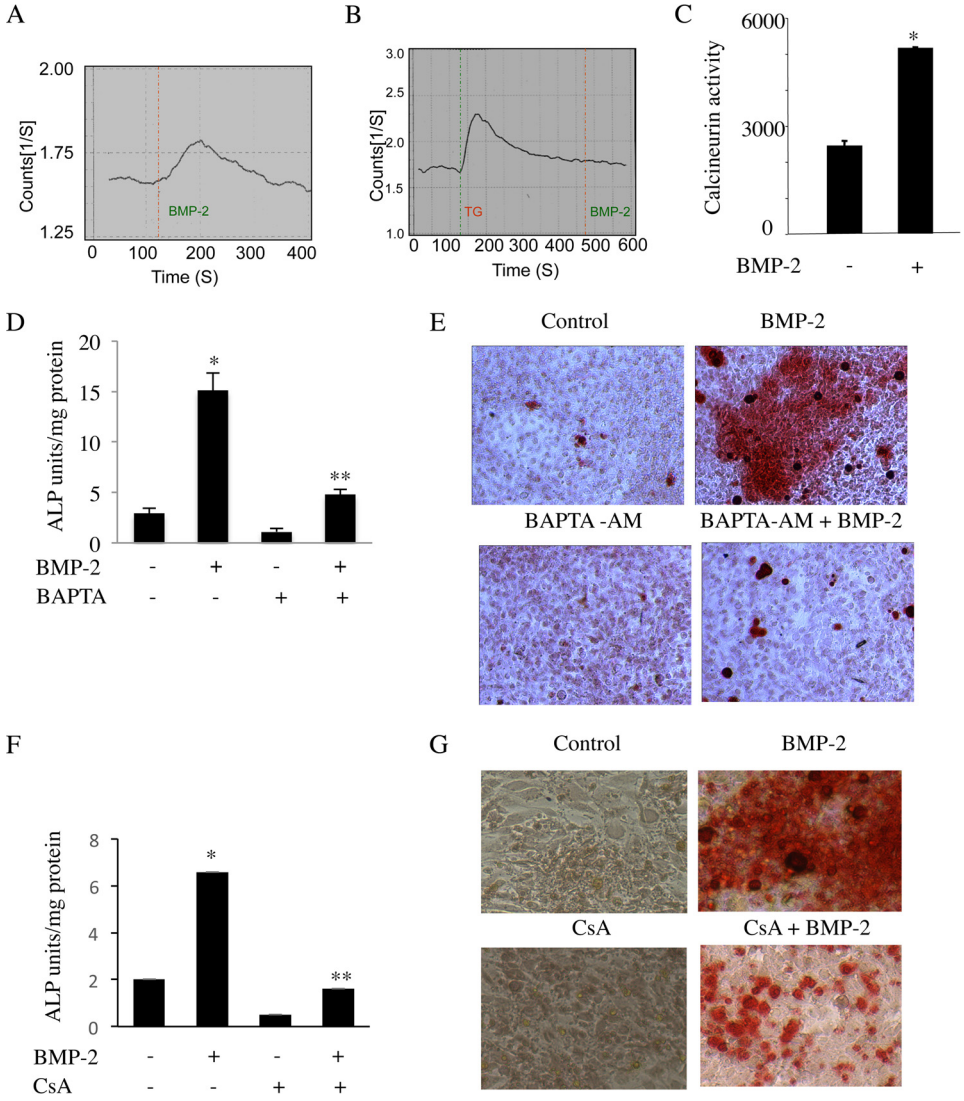

FIGURE 6. **BMP-2-induced intracellular Ca^{2+} release and calcineurin phosphatase activity are critical for osteoblast differentiation.** *A* and *B*, Ca^{2+} release was measured in C2C12 cells in response to BMP-2 in the presence (*B*) or absence (*A*) of thapsigargin (*TG*). *C*, calcineurin activity was determined in C2C12 cells in response to BMP-2 at 24 h as described under "Experimental Procedures." Mean ± S.E. of triplicate determinations is shown. *, $p < 0.01$ *versus* control. *D–G*, Ca^{2+} and calcineurin activity are required for BMP-2-mediated osteoblast differentiation. C2C12 cells were treated with BAPTA-AM (*D* and *E*) or CsA (*F* and *G*) followed by BMP-2 in osteoblastic differentiation medium. Cells were either harvested at 48 h for alkaline phosphatase (*ALP*) assay (*D* and *F*) or stained for mineralized nodule formation after 12 days (*E* and *G*). For *D* and *F*, mean ± S.E. of six measurements is shown. *, $p < 0.001$ *versus* control; **, $p < 0.001$ *versus* BMP-2-treated. *Error bars* represent S.E.

the selective endoplasmic reticulum Ca^{2+} pump inhibitor thapsigargin, which promotes depletion of intracellular Ca^{2+} (Fig. 6*B*). NFATc1 activation requires Ca^{2+}-dependent calcineurin phosphatase activity. Therefore, we analyzed the effect of BMP-2 on calcineurin phosphatase activity in C2C12 cells using an *in vitro* phosphatase assay (40). Treatment with BMP-2 resulted in a 2-fold increase in calcineurin activity (Fig. 6*C*).

BMP-2 induces differentiation of C2C12 cells into matured osteoblasts. Our results above demonstrate a role of BMP-2 in Ca^{2+} release from the intracellular store and activation of calcineurin. Therefore, we first examined the role of Ca^{2+} in osteoblast differentiation using the intracellular Ca^{2+} chelator BAPTA-AM. Expression of alkaline phosphatase acts as a marker for osteoblast differentiation. BMP-2 increased alkaline phosphatase activity in C2C12 cells (Fig. 6*D*). Treatment of these cells with BAPTA-AM prior to incubation with BMP-2 significantly inhibited the BMP-2-stimulated alkaline phosphatase activity (Fig. 6*D*). Consequently, BAPTA-AM abrogated BMP-2-induced differentiation of C2C12 cells into mature osteoblasts as judged by Alizarin Red assay (Fig. 6*E*). Similarly, cyclosporin A (CsA), a pharmacological inhibitor of calcineurin, blocked BMP-2-mediated alkaline phosphatase activity and osteoblast differentiation (Fig. 6*F* and 6*G*). These results indicate a requirement for Ca^{2+}-calcineurin, which may regulate BMP-2-induced NFATc1 expression for osteoblast differentiation.

Ca^{2+}/Calcineurin Signaling Contributes to BMP-2-stimulated NFATc1 Expression and Autoregulation—To determine the involvement of calcineurin phosphatase activity in BMP-2-induced NFATc1 expression, we used CsA. CsA abolished the BMP-2-mediated increase in expression of NFATc1 protein

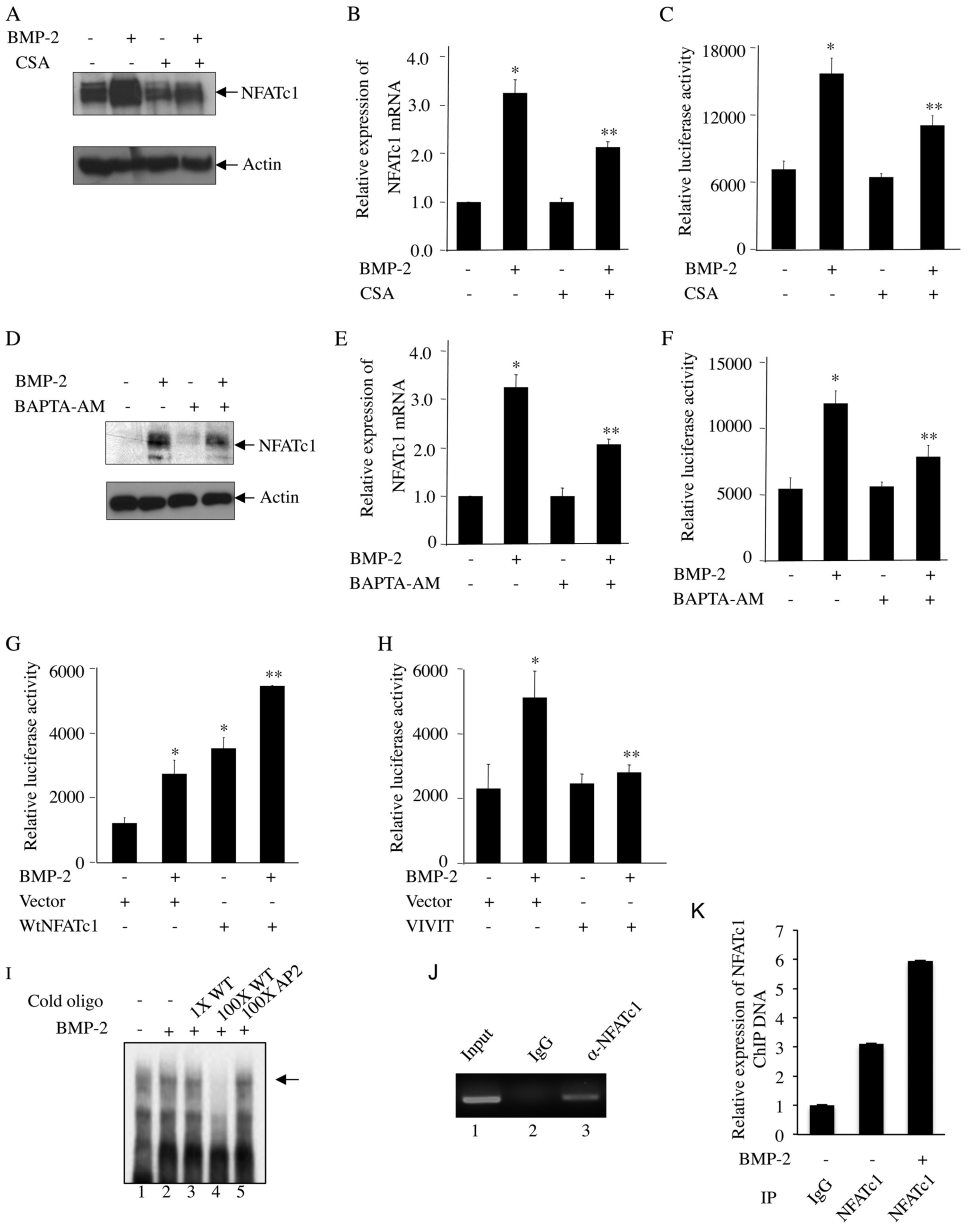

FIGURE 7. **BMP-2-induced autoregulation of NFATc1.** *A–F*, BMP-2-mediated NFATc1 expression requires Ca^{2+}/calcineurin signaling in osteoblasts. C2C12 cells were pretreated with CsA (*A–C*) or BAPTA-AM (*D–F*) followed by incubation with BMP-2. NFATc1 protein (*A* and *D*) or mRNA (*B* and *E*) expression and transcriptional activity (*C* and *F*) were analyzed by immunoblotting with NFATc1 and actin antibodies, qRT-PCR analysis, or luciferase activity assay as described in Fig. 2, *B*, *C*, and *D*, respectively. For *B*, *C*, *E*, and *F*, mean ± S.E. of quadruplicate measurements is shown. *, $p < 0.001$ *versus* control; **, $p < 0.01$ *versus* BMP-2-treated. *G*, NFATc1 promoter activity is induced by NFATc1 expression. C2C12 cells were cotransfected with NFATc1-Luc plasmid and NFATc1 expression plasmid followed by incubation with BMP-2. Luciferase activity was measured in the cell lysates as described in Fig. 2*D*. *H*, inhibition of NFATc1 activity by VIVIT blocks BMP-2-mediated NFATc1 promoter activity. C2C12 cells were transfected with VIVIT expression plasmid together with NFATc1-Luc followed by BMP-2 treatment. Luciferase activity was determined in the cell lysates as described in Fig. 2*D*. For *G* and *H*, mean ± S.E. of triplicate measurements is shown. *, $p < 0.01$ *versus* control; **, $p < 0.01$ *versus* BMP-2-treated. *I–K*, BMP-2 increases interaction of NFATc1 with NFATc1 P1 promoter at −700 bp. Nuclear extracts from C2C12 cells treated with BMP-2 were analyzed by EMSA using radiolabeled NFATc1 probe spanning −700 to −661 bp as described under "Experimental Procedures" (*I*). Cold oligonucleotide probe for NFATc1 (*lanes 3* and *4*) or AP2 (*lane 5*) was used in EMSA. *J* and *K*, ChIP assay was used to detect NFATc1 binding as described under "Experimental Procedures." *Error bars* represent S.E. *IP*, immunoprecipitation.

and mRNA (Fig. 7, *A* and *B*). Similarly, BMP-2-induced transcription of NFATc1 was also inhibited by CsA (Fig. 7*C*). The intracellular Ca^{2+} chelator BAPTA-AM blocked BMP-2-induced NFATc1 protein and mRNA expression and its transcriptional activation (Fig. 7, *D*, *E*, and *F*), indicating an inherent role of Ca^{2+} in BMP-2-induced NFATc1 expression. To directly investigate the involvement of NFATc1 in its transcription, we cotransfected the cells with NFATc1 promoter-luciferase reporter plasmid (NFATc1-Luc) and the NFATc1 expression vector. Incubation of these cells with BMP-2 increased the transcription of NFATc1. However, expression of NFATc1 significantly increased the transcription similarly to that obtained with BMP-2 (Fig. 7*G*). Both BMP-2 and NFATc1 had an additive effect on NFATc1 transcription (Fig. 7*G*). Conversely, expression of VIVIT peptide, a specific inhibitor of NFATc1, blocked BMP-2-induced transcription of NFATc1 (Fig. 7*H*). NFATc1 was shown to bind to NFATc1 P1 promoter and autoregulate its own transcription (33). To test the association of

NFATc1 with NFATc1 P1 promoter in osteoblasts, we used an oligonucleotide for NFAT binding element spanning −700 to −661 bp as described by Chuvpilo *et al.* (33) in an electrophoretic mobility shift assay. DNA-protein interaction was observed using nuclear extract isolated from osteoblast cells (Fig. 7*I*, *lane 1*), and this was increased by BMP-2 treatment (Fig. 7*I*, compare *lane 2* with *lane 1*). The specificity of this DNA-protein interaction was confirmed by incubating with cold oligonucleotide that was used as radioactive probe in this assay. Incubation of the nuclear extract with 100-fold excess cold NFATc1 oligonucleotide probe followed by radioactively labeled probe in this assay abolished association of radioactive probe with the nuclear protein (Fig. 7*I*, compare *lane 4* with *lane 2*). Incubation with a 100-fold excess of a nonspecific oligonucleotide did not alter the specific association of radiolabeled NFATc1 probe with osteoblastic nuclear proteins (Fig. 7*I*, compare *lane 5* with *lane 2*). Interaction of NFATc1 with NFAT P1 promoter in osteoblasts was confirmed using a ChIP assay. The ChIP assay with NFATc1 antibody and subsequent PCR using primers specific for the NFATc1 binding sites in P1 promoter confirmed binding of NFATc1 with P1 promoter (Fig. 7*J*). BMP-2 treatment augmented this interaction of NFATc1 on P1 promoter (Fig. 7*K*). These results suggest a role of Ca^{2+}-dependent calcineurin in BMP-2-mediated expression of NFATc1, which in turn feeds forward to autoregulate its expression.

Discussion

Bone remodeling is controlled by cooperative actions of osteoblasts and osteoclasts. The calcium-sensitive NFATc1 transcription factor regulates osteoclast differentiation downstream of the osteoblast-coded factors RANKL and CSF-1, expression of which is in turn controlled by BMP-2 (12, 18, 19, 41). Our study shows the presence of an autoregulatory loop for NFATc1 expression in BMP-2-stimulated osteoblasts that drives their differentiation. Moreover, our study identified a novel role of BMP-2 in stimulating intracellular Ca^{2+} release and calcineurin phosphatase activity necessary for NFATc1 gene expression in osteoblasts. Additionally, BMP-2 integrates its receptor-specific Smad pathway and PI 3-kinase/Akt signaling to induce expression of NFATc1 and its nuclear translocation in osteoblast cells (Fig. 8).

Mice overexpressing the constitutively activated form of NFATc1 in osteoblasts developed a high bone mass phenotype resulting from increased osteoblast function (13). As a possible mechanism, it was demonstrated that NFATc1 functions in recruiting osteoclast progenitors by increasing chemoattractant production by osteoblasts (13). Studies from mice treated with the calcineurin inhibitor FK506 showed a decrease in osteoclast number and activity leading to decreased bone resorption. Surprisingly, FK506 treatment also decreased trabecular bone volume, indicating a role of NFATc1 in osteoblastic bone formation (41). A similar bone phenotype of low bone mass was observed in BMP-2 cKO mice (38). Immunohistochemical staining of trabecular bone sections from these BMP-2 cKO mice showed significant reduction in NFATc1 expression (Fig. 1*L*). Indeed, BMP-2 was found to induce NFATc1 mRNA and protein expression in osteoblast cells in a dose- and time-dependent manner (Fig. 1, *A*–*G*).

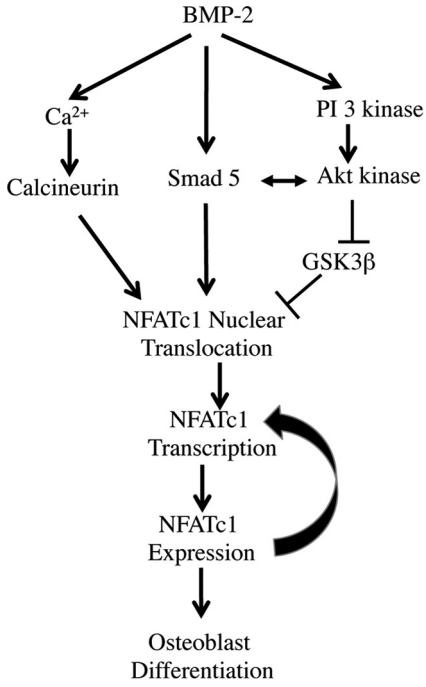

FIGURE 8. **A schematic representation of the findings described in this study.**

Regulation of NFATc1 expression has been extensively studied in T lymphocytes in response to antigen exposure. In these cells, NFATc1 is synthesized in three isoforms due to differential use of the polyadenylation sites (42). As an additional control mechanism, two distinct promoters, namely P1 and P2, regulate NFATc1 expression in T lymphocytes (33). The P1 promoter contains binding sites for a number of transcription factors and resides within a CpG island proximal to exon 1 of NFATc1 gene. P1 promoter is hypermethylated in kidney cells where NFATc1 is not expressed and is demethylated in effector T cells with increased NFATc1 expression (33). The studies conducted by the same group identified a binding region for a number of transcription factors including NFκB, Sp1, Sp3, and NFAT within the 800-bp P1 promoter. Coordinated interaction of these factors with P1 promoter regulates NFATc1 expression in the effector T cells. We show that BMP-2 preferentially stimulated NFATc1 mRNA expression from P1 promoter, whereas the P2 promoter remained unresponsive to BMP-2 in the preosteoblast cells (Fig. 1, *J* and *K*). Autoregulation of NFATc1, driven by the two NFATc1 binding regions in P1 promoter, was identified in effector T lymphocytes (33). We explored the possibility of NFATc1 promoter autoregulation in osteoblast cells and demonstrated robust stimulation of the P1 promoter activity by NFATc1 that is further augmented by treatment with BMP-2, acting by facilitating NFATc1 nuclear import (Fig. 3, *F* and *G*). We show that BMP-2-mediated NFATc1 autoregulatory function in osteoblasts was due to direct association of NFATc1 with NFATc1 P1 promoter at the NFATc1 binding site (Fig. 7, *I*, *J*, and *K*) (33). This observation for the first time demonstrates that BMP-2 selectively targets P1 promoter to induce NFATc1 expression, which in turn feeds forward to further potentiate its own expression in osteoblasts.

BMP-2 orchestrates signaling through Smad proteins for regulating expression of osteoblastic genes necessary for the

osteoblast differentiation program (30). BMP-2-induced NFATc1 expression and nuclear localization were blocked by exogenous expression of the inhibitory Smad6 that targets BMP-specific Smad signaling (Figs. 2 and 3), indicating a direct role of Smads in osteoblastic expression and activation of NFATc1. We have established a requirement for PI 3-kinase and its downstream target Akt kinase in BMP-2-mediated osteoblast differentiation (25). Using expression plasmids for PTEN and dominant negative Akt kinase along with a pharmacological inhibitor for PI 3-kinase activity (Ly294002), we confirmed the involvement of the PI 3-kinase/Akt signaling pathway for NFATc1 protein and mRNA expression in BMP-2-stimulated preosteoblast cells (Fig. 4).

Different signaling pathways communicate and cooperate to maintain the fine balance in gene expression. Such a signaling cross-talk exists between PI 3-kinase/Akt and Smad signaling in BMP-2-mediated CSF-1 gene expression in osteoblast cells (15). We show that BMP-2-mediated NFATc1 expression also required cooperative inputs from Smad and PI 3-kinase/Akt signaling (Fig. 5, *G* and *H*). Toward this signaling cross-talk, we show that BMP-2 induced association of Akt and Smad1/5 in osteoblasts (Fig. 5, *E* and *F*). In T cells, activation and nuclear import of NFATc1 require dephosphorylation by calcineurin, whereas GSK3β phosphorylates and expels NFATc1 from the nucleus (9, 27). Activity of GSK3β is inhibited by phosphorylation at the Ser-9 residue (43). Akt kinase directly phosphorylates and inactivates GSK3β in response to insulin (28). We previously showed that BMP-2 activates Akt kinase in osteoblasts (25). Here we show that BMP-2 increased phosphorylation of GSK3β in Akt-dependent manner (Fig. 5, *A–C*). Phosphorylation of GSK3β also increased nuclear accumulation of NFATc1 (Fig. 5*D*), thus facilitating NFATc1 autoregulation and transcriptional activation. Taken together, we identified a mechanism through which BMP-2-induced Akt activation results in increased expression of NFATc1 in osteoblasts.

Calcium signaling plays a key role in osteoblast proliferation and differentiation. Parathyroid hormone and vitamin D_3 increase intracellular Ca^{2+} concentrations in osteoblasts by mobilizing Ca^{2+} stored in intracellular organelles (44, 45). Both TGFβ and BMP-2 enhance adhesion of human osteoblast cells to biomaterials and thus improve the functionality of orthopedic implants (46). Intracellular Ca^{2+} signaling plays an essential role in TGFβ-induced increased adhesion of human osteoblast cells (47). In pulmonary arterial smooth muscle cells, although BMP-4 induces an intracellular Ca^{2+} increase, BMP-2 was found to inhibit it (48, 49). This observation explained the opposing functions of BMP-4 and BMP-2 toward chronic hypoxic pulmonary hypertension where BMP-2 plays the preventative role and BMP-4 promotes vascular remodeling. We found BMP-2 to induce a rapid and transient rise in intracellular Ca^{2+} that was blocked when the cells were treated with the endoplasmic reticulum-specific Ca^{2+} pump inhibitor thapsigargin (Fig. 6, *A* and *B*). The importance of Ca^{2+} signaling in BMP-2-induced osteoblastic gene expression and osteoblast differentiation is unknown. Based on the fact that NFATc1 activation depends on Ca^{2+}-directed calcineurin phosphatase activity, we measured calcineurin phosphatase activity in osteoblast cells treated with BMP-2. We found induction of calcineurin phosphatase activity in preosteoblasts in response to BMP-2 (Fig. 6*C*). Blocking of intracellular Ca^{2+} release by BAPTA-AM or inhibiting calcineurin activity by CsA dampened BMP-2-induced alkaline phosphatase activity and mineralized nodule formation in these cells (Fig. 6, *D–G*). This confirms a direct involvement of Ca^{2+}-driven calcineurin activity in BMP-2-mediated osteoblast differentiation. In addition, BAPTA-AM and CsA inhibited BMP-2-induced NFATc1 protein and mRNA expression (Fig. 7, *A–F*), indicating a requirement of Ca^{2+} signaling and calcineurin phosphatase activity for BMP-2-mediated NFATc1 expression in these cells.

In summary, we report here a novel mechanism of osteoblastic NFATc1 expression and autoregulation in response to BMP-2 that involves orchestration of signaling pathways involving Ca^{2+}, Smads, and PI 3-kinase/Akt (Fig. 8). Also we provide evidence for the involvement of Ca^{2+}/calcineurin signaling in osteoblast differentiation downstream of BMP-2. Whether BMP-2-mediated Ca^{2+} signaling plays a role in the Smad and PI 3-kinase signaling pathway in relation to bone remodeling will be of interest and will need further investigation.

Author Contributions—The experiments were mainly performed by C. C. M. with substantial contribution from F. D. S. G. performed immunohistochemical analysis. S. E. H. provided the BMP-2 cKO mice for this study. G. G. C. provided critical input in designing experiments, data analyses, and manuscript preparation. N. G.-C. formulated the study, analyzed data, and prepared the manuscript.

References

1. Capulli, M., Paone, R., and Rucci, N. (2014) Osteoblast and osteocyte: games without frontiers. *Arch. Biochem. Biophys.* **561,** 3–12
2. Negishi-Koga, T., and Takayanagi, H. (2009) Ca^{2+}-NFATc1 signaling is an essential axis of osteoclast differentiation. *Immunol. Rev.* **231,** 241–256
3. Eapen, A., Sundivakkam, P., Song, Y., Ravindran, S., Ramachandran, A., Tiruppathi, C., and George, A. (2010) Calcium-mediated stress kinase activation by DMP1 promotes osteoblast differentiation. *J. Biol. Chem.* **285,** 36339–36351
4. Blair, H. C., Robinson, L. J., Huang, C. L., Sun, L., Friedman, P. A., Schlesinger, P. H., and Zaidi, M. (2011) Calcium and bone disease. *Biofactors* **37,** 159–167
5. Takahashi, N., Akatsu, T., Udagawa, N., Sasaki, T., Yamaguchi, A., Moseley, J. M., Martin, T. J., and Suda, T. (1988) Osteoblastic cells are involved in osteoclast formation. *Endocrinology* **123,** 2600–2602
6. Takami, M., Takahashi, N., Udagawa, N., Miyaura, C., Suda, K., Woo, J. T., Martin, T. J., Nagai, K., and Suda, T. (2000) Intracellular calcium and protein kinase C mediate expression of receptor activator of nuclear factor-κB ligand and osteoprotegerin in osteoblasts. *Endocrinology* **141,** 4711–4719
7. Lee, H. L., Bae, O. Y., Baek, K. H., Kwon, A., Hwang, H. R., Qadir, A. S., Park, H. J., Woo, K. M., Ryoo, H. M., and Baek, J. H. (2011) High extracellular calcium-induced NFATc3 regulates the expression of receptor activator of NF-κB ligand in osteoblasts. *Bone* **49,** 242–249
8. Shaw, J. P., Utz, P. J., Durand, D. B., Toole, J. J., Emmel, E. A., and Crabtree, G. R. (1988) Identification of a putative regulator of early T cell activation genes. *Science* **241,** 202–205
9. Beals, C. R., Clipstone, N. A., Ho, S. N., and Crabtree, G. R. (1997) Nuclear localization of NF-ATc by a calcineurin-dependent, cyclosporin-sensitive intramolecular interaction. *Genes Dev.* **11,** 824–834
10. Koga, T., Matsui, Y., Asagiri, M., Kodama, T., de Crombrugghe, B., Nakashima, K., and Takayanagi, H. (2005) NFAT and Osterix cooperatively regulate bone formation. *Nat. Med.* **11,** 880–885

11. Asagiri, M., and Takayanagi, H. (2007) The molecular understanding of osteoclast differentiation. *Bone* **40,** 251–264
12. Takayanagi, H., Kim, S., Koga, T., Nishina, H., Isshiki, M., Yoshida, H., Saiura, A., Isobe, M., Yokochi, T., Inoue, J., Wagner, E. F., Mak, T. W., Kodama, T., and Taniguchi, T. (2002) Induction and activation of the transcription factor NFATc1 (NFAT2) integrate RANKL signaling in terminal differentiation of osteoclasts. *Dev. Cell* **3,** 889–901
13. Winslow, M. M., Pan, M., Starbuck, M., Gallo, E. M., Deng, L., Karsenty, G., and Crabtree, G. R. (2006) Calcineurin/NFAT signaling in osteoblasts regulates bone mass. *Dev. Cell* **10,** 771–782
14. Ikeda, F., Nishimura, R., Matsubara, T., Tanaka, S., Inoue, J., Reddy, S. V., Hata, K., Yamashita, K., Hiraga, T., Watanabe, T., Kukita, T., Yoshioka, K., Rao, A., and Yoneda, T. (2004) Critical roles of c-Jun signaling in regulation of NFAT family and RANKL-regulated osteoclast differentiation. *J. Clin. Investig.* **114,** 475–484
15. Mandal, C. C., Ghosh Choudhury, G., and Ghosh-Choudhury, N. (2009) Phosphatidylinositol 3 kinase/Akt signal relay cooperates with Smad in bone morphogenetic protein-2-induced colony stimulating factor-1 (CSF-1) expression and osteoclast differentiation. *Endocrinology* **150,** 4989–4998
16. Manolagas, S. C., and Jilka, R. L. (1995) Bone marrow, cytokines, and bone remodeling. Emerging insights into the pathophysiology of osteoporosis. *New Engl. J. Med.* **332,** 305–311
17. Olsen, B. R., Reginato, A. M., and Wang, W. (2000) Bone development. *Annu. Rev. Cell Dev. Biol.* **16,** 191–220
18. Ghosh-Choudhury, N., Singha, P. K., Woodruff, K., St Clair, P., Bsoul, S., Werner, S. L., and Choudhury, G. G. (2006) Concerted action of Smad and CREB-binding protein regulates bone morphogenetic protein-2-stimulated osteoblastic colony-stimulating factor-1 expression. *J. Biol. Chem.* **281,** 20160–20170
19. Itoh, K., Udagawa, N., Katagiri, T., Iemura, S., Ueno, N., Yasuda, H., Higashio, K., Quinn, J. M., Gillespie, M. T., Martin, T. J., Suda, T., and Takahashi, N. (2001) Bone morphogenetic protein 2 stimulates osteoclast differentiation and survival supported by receptor activator of nuclear factor-κB ligand. *Endocrinology* **142,** 3656–3662
20. Abe, E., Yamamoto, M., Taguchi, Y., Lecka-Czernik, B., O'Brien, C. A., Economides, A. N., Stahl, N., Jilka, R. L., and Manolagas, S. C. (2000) Essential requirement of BMPs-2/4 for both osteoblast and osteoclast formation in murine bone marrow cultures from adult mice: antagonism by noggin. *J. Bone Miner. Res.* **15,** 663–673
21. Macías-Silva, M., Hoodless, P. A., Tang, S. J., Buchwald, M., and Wrana, J. L. (1998) Specific activation of Smad1 signaling pathways by the BMP7 type I receptor, ALK2. *J. Biol. Chem.* **273,** 25628–25636
22. ten Dijke, P., Yamashita, H., Sampath, T. K., Reddi, A. H., Estevez, M., Riddle, D. L., Ichijo, H., Heldin, C. H., and Miyazono, K. (1994) Identification of type I receptors for osteogenic protein-1 and bone morphogenetic protein-4. *J. Biol. Chem.* **269,** 16985–16988
23. Attisano, L., and Wrana, J. L. (2000) Smads as transcriptional co-modulators. *Curr. Opin. Cell Biol.* **12,** 235–243
24. Massagué, J., and Chen, Y. G. (2000) Controlling TGF-β signaling. *Genes Dev.* **14,** 627–644
25. Ghosh-Choudhury, N., Abboud, S. L., Nishimura, R., Celeste, A., Mahimainathan, L., and Choudhury, G. G. (2002) Requirement of BMP-2-induced phosphatidylinositol 3-kinase and Akt serine/threonine kinase in osteoblast differentiation and Smad-dependent BMP-2 gene transcription. *J. Biol. Chem.* **277,** 33361–33368
26. Takayanagi, H. (2007) The role of NFAT in osteoclast formation. *Ann. N.Y. Acad. Sci.* **1116,** 227–237
27. Beals, C. R., Sheridan, C. M., Turck, C. W., Gardner, P., and Crabtree, G. R. (1997) Nuclear export of NF-ATc enhanced by glycogen synthase kinase-3. *Science* **275,** 1930–1934
28. Cross, D. A., Alessi, D. R., Cohen, P., Andjelkovich, M., and Hemmings, B. A. (1995) Inhibition of glycogen synthase kinase-3 by insulin mediated by protein kinase B. *Nature* **378,** 785–789
29. Ghosh-Choudhury, N., Windle, J. J., Koop, B. A., Harris, M. A., Guerrero, D. L., Wozney, J. M., Mundy, G. R., and Harris, S. E. (1996) Immortalized murine osteoblasts derived from BMP 2-T-antigen expressing transgenic mice. *Endocrinology* **137,** 331–339
30. Mandal, C. C., Drissi, H., Choudhury, G. G., and Ghosh-Choudhury, N. (2010) Integration of phosphatidylinositol 3-kinase, Akt kinase, and Smad signaling pathway in BMP-2-induced osterix expression. *Calcif. Tissue Int.* **87,** 533–540
31. Mandal, C. C., Ganapathy, S., Gorin, Y., Mahadev, K., Block, K., Abboud, H. E., Harris, S. E., Ghosh-Choudhury, G., and Ghosh-Choudhury, N. (2011) Reactive oxygen species derived from Nox4 mediate BMP2 gene transcription and osteoblast differentiation. *Biochem. J.* **433,** 393–402
32. Mandal, C. C., Ghosh-Choudhury, T., Dey, N., Choudhury, G. G., and Ghosh-Choudhury, N. (2012) miR-21 is targeted by ω-3 polyunsaturated fatty acid to regulate breast tumor CSF-1 expression. *Carcinogenesis* **33,** 1897–1908
33. Chuvpilo, S., Jankevics, E., Tyrsin, D., Akimzhanov, A., Moroz, D., Jha, M. K., Schulze-Luehrmann, J., Santner-Nanan, B., Feoktistova, E., König, T., Avots, A., Schmitt, E., Berberich-Siebelt, F., Schimpl, A., and Serfling, E. (2002) Autoregulation of NFATc1/A expression facilitates effector T cells to escape from rapid apoptosis. *Immunity* **16,** 881–895
34. Ghosh-Choudhury, N., Mandal, C. C., and Choudhury, G. G. (2007) Statin-induced Ras activation integrates the phosphatidylinositol 3-kinase signal to Akt and MAPK for bone morphogenetic protein-2 expression in osteoblast differentiation. *J. Biol. Chem.* **282,** 4983–4993
35. Ghosh-Choudhury, N., Mandal, C. C., Das, F., Ganapathy, S., Ahuja, S., and Ghosh Choudhury, G. (2013) c-Abl-dependent molecular circuitry involving Smad5 and phosphatidylinositol 3-kinase regulates bone morphogenetic protein-2-induced osteogenesis. *J. Biol. Chem.* **288,** 24503–24517
36. Mandal, C. C., Ghosh-Choudhury, N., Yoneda, T., Choudhury, G. G., and Ghosh-Choudhury, N. (2011) Simvastatin prevents skeletal metastasis of breast cancer by an antagonistic interplay between p53 and CD44. *J. Biol. Chem.* **286,** 11314–11327
37. Zhang, G. H., Helmke, R. J., and Martinez, J. R. (1997) Characterization of Ca^{2+} mobilization in the human submandibular duct cell line A253. *Proc. Soc. Exp. Biol. Med.* **216,** 117–124
38. Yang, W., Guo, D., Harris, M. A., Cui, Y., Gluhak-Heinrich, J., Wu, J., Chen, X. D., Skinner, C., Nyman, J. S., Edwards, J. R., Mundy, G. R., Lichtler, A., Kream, B. E., Rowe, D. W., Kalajzic, I., David, V., Quarles, D. L., Villareal, D., Scott, G., Ray, M., Liu, S., Martin, J. F., Mishina, Y., and Harris, S. E. (2013) Bmp2 in osteoblasts of periosteum and trabecular bone links bone formation to vascularization and mesenchymal stem cells. *J. Cell Sci.* **126,** 4085–4098
39. Cantley, L. C., and Neel, B. G. (1999) New insights into tumor suppression: PTEN suppresses tumor formation by restraining the phosphoinositide 3-kinase/AKT pathway. *Proc. Natl. Acad. Sci. U.S.A.* **96,** 4240–4245
40. Fruman, D. A., Pai, S. Y., Klee, C. B., Burakoff, S. J., and Bierer, B. E. (1996) Measurement of calcineurin phosphatase activity in cell extracts. *Methods* **9,** 146–154
41. Koga, T., Inui, M., Inoue, K., Kim, S., Suematsu, A., Kobayashi, E., Iwata, T., Ohnishi, H., Matozaki, T., Kodama, T., Taniguchi, T., Takayanagi, H., and Takai, T. (2004) Costimulatory signals mediated by the ITAM motif cooperate with RANKL for bone homeostasis. *Nature* **428,** 758–763
42. Chuvpilo, S., Zimmer, M., Kerstan, A., Glöckner, J., Avots, A., Escher, C., Fischer, C., Inashkina, I., Jankevics, E., Berberich-Siebelt, F., Schmitt, E., and Serfling, E. (1999) Alternative polyadenylation events contribute to the induction of NF-ATc in effector T cells. *Immunity* **10,** 261–269
43. Sutherland, C., Leighton, I. A., and Cohen, P. (1993) Inactivation of glycogen synthase kinase-3β by phosphorylation: new kinase connections in insulin and growth-factor signalling. *Biochem. J.* **296,** 15–19
44. Boden, S. D., and Kaplan, F. S. (1990) Calcium homeostasis. *Orthop. Clin. North Am.* **21,** 31–42
45. Dvorak, M. M., and Riccardi, D. (2004) Ca^{2+} as an extracellular signal in bone. *Cell Calcium* **35,** 249–255
46. Shah, A. K., Lazatin, J., Sinha, R. K., Lennox, T., Hickok, N. J., and Tuan, R. S. (1999) Mechanism of BMP-2 stimulated adhesion of osteoblastic cells to titanium alloy. *Biol. Cell* **91,** 131–142
47. Nesti, L. J., Caterson, E. J., Li, W. J., Chang, R., McCann, T. D., Hoek, J. B.,

and Tuan, R. S. (2007) TGF-β1 calcium signaling in osteoblasts. *J. Cell. Biochem.* **101,** 348–359

48. Zhang, Y., Lu, W., Yang, K., Xu, L., Lai, N., Tian, L., Jiang, Q., Duan, X., Chen, M., and Wang, J. (2013) Bone morphogenetic protein 2 decreases TRPC expression, store-operated Ca^{2+} entry, and basal $[Ca^{2+}]_i$ in rat distal pulmonary arterial smooth muscle cells. *Am. J. Physiol. Cell Physiol.* **304,** C833–C843
49. Lu, W., Ran, P., Zhang, D., Lai, N., Zhong, N., and Wang, J. (2010) Bone morphogenetic protein 4 enhances canonical transient receptor potential expression, store-operated Ca^{2+} entry, and basal $[Ca^{2+}]_i$ in rat distal pulmonary arterial smooth muscle cells. *Am. J. Physiol. Cell Physiol.* **299,** C1370–C1378